ENGINEERING TRANSACTIONS • *Engng. Trans.* • **47**, 2, 99–115, 1999
Polish Academy of Sciences • Institute of Fundamental Technological Research
10.24423/engtrans.619.1999

NONLINEAR FINITE ELEMENT ANALYSIS OF BONE-CEMENT INTERFACE CONDITION IN CEMENTED TOTAL HIP REPLACEMENT

P. COLOMBI

DEPARTMENT OF STRUCTURAL ENGINEERING,
MILAN UNIVERSITY OF TECHNOLOGY
Milan, Italy

and

L. SGAMBI

MS student at the "School for the Design of R/C Structures",
MILAN UNIVERSITY OF TECHNOLOGY
Milan, Italy

Loosening of cemented femoral hip component is one of the major failure mode in cemented total hip arthroplasty. The stem-cement and bone-cement interface conditions strongly influence the load transfer mechanism in the implant system and then the stress distribution in the bone, the stem and cement mantle. Nonlinear Coulomb friction model was often used in the literature to study the stem-cement interface. On the other hand, the bone-cement interface was usually considered to be bonded, and a tissue layer between the bone and the cement was introduced to model the long-term behaviour of a total hip arthroplasty. More recently, experimental investigations were carried out to study the general mechanical behaviour of the bone-cement interface under tensile or shear loading. Under tensile loading, the results showed that the post-yield tensile behaviour contributed substantially to the energy required to produce the failure of the bone-cement interface. Moreover the post-yield behaviour showed a positive correlation with the amount of interdigitation or bone density. The goal of this paper is to introduce a microstructural model based on a continuum damage mechanics for studying the bone-cement interface conditions. The present study is limited to the tensile behaviour since more detailed experimental data are available in this particular case. The numerical results show a good agreement with the experimental one and represent a first step toward the study of the bone-cement interface under combined normal and shear loading.

1. INTRODUCTION

Femoral component loosening continues to be a major mode of failure in cemented total hip arthroplasty. Radiolucent lines at the bone-cement and stem-cement interface, resorption of the bone surrounding the cement mantle and fracture of the cement mantle have been associated with clinical loosening of femoral components (MANN *et al.*, [5]). To this end, a mechanical failure mechanism involving the stem-cement and bone-cement interface has been hypothesised. The finite element method has been used extensively to study the load transfer between the stem, cement and bone. The goals of most of these investigations were to evaluate if the predicted stress levels in the finite element models were large enough to result in failure of a component of the system and to determine the design parameters that affect the stress level. Several models have assumed displacement compatibility at the bone-cement and stem-cement interfaces and then a perfect bond. More recently (MANN *et al.*, [5]), finite element analyses have been performed that assume a more realistic interface conditions between the stem and the bone. Sometimes, a fibrous tissue layer at the bone-cement interface has been assumed to model the long-term interface condition (WEINANS *et al.*, [12]).

A more realistic bone-cement interface conditions, including the normal and shear stresses at the interface, should be taken into account in order to model the early post-op conditions. Because the bone and the cement interdigitate, there is not a unique interface between them. Instead there is a composite region of cancellous bone and cement which cooperate with cancellous bone on one side and with the cement on the other. Clinical evidence (JASTY *et al.*, [4]) shows that retrieved specimen at less than 5 years post-op had no fibrous tissue formation and trabecular bone that was well interdigitated within the cement. In (MANN *et al.*, [6]) an experimental investigation of the cement-bone interface tensile behaviour was performed. Under displacement-controlled tensile loading of the cement-bone interface, there were no abrupt failures after the peak tensile loading was reached. Rather a large amount of strain softening occurred with a substantial amount of energy absorbed by the failing interface. The mechanical properties of the interface were related to the bone density at the interface and to the amount of cement-bone interdigitation. In MANN *et al.*, [7], a non linear fracture mechanics model was introduced to reproduce the behaviour of experimental bone-cement tests specimen and an idealised stem-cement-bone structure. They found a strong dependence of the structure stiffness on the interface behaviour but this idealised situation is maybe too far from a realistic implant. FUNK *et al.*, [3] performed shear tests on bone-cement interface using two types of cement, standard polymethylmethacrylate (PMMA) and a reduced modulus formulation

with polybutylmethacrylate (PBMMA). Strength and modulus were dictated by the bone at the bone-composite interface. Unfortunately, no data were indicated on the bone density and no load-displacement plots were reported by the authors. This paper is limited to standard PMMA, so the properties of this type of cement will be used throughout this work.

The goal of this paper is to introduce a microstructural model based on continuum damage mechanics approach to study the tensile behaviour of the cement-bone interface. The study is limited to tensile loading since detailed experimental data are available in the literature only for this particular loading case. First, a quasi-three-dimensional finite element model of the prosthesis implant will be introduced in order to study the stress distribution at the stem-cement and bone-cement interface, and the effect of the stem-cement frictional properties. MANN *et al.*, [6] recognised that the tensile failure of the interface occurs by failure of the trabeculae at the extent of cement penetration, and that the strength is maximised by increasing the amount of trabecular bone in the cement. These findings suggest that the mechanism of trabecular bone failure is similar to the interfacial failure. Then, a micro-mechanical model (COLOMBI *et al.*, [2]) previously developed to study the tensile behaviour of bulk trabecular bone specimens was used to reproduce the tensile test curve of the bone-cement interface. However, the actual behaviour of the bone-cement interface should include also the shear or combined normal and shear failure model (MANN *et al.*, [7]). Therefore this paper is a preliminary step toward the study of a more realistic model for bone-cement interface model in the early post-op period.

2. METHODS

A quasi-three-dimensional (WEINANS *et al.*, [1]) FEM model of the femoral hip arthroplasty was constructed in order to study the stress distribution at the stem-cement and bone cement-interface in a early post-op situation. No fibrous tissue membrane was inserted and modelled in the finite element analysis. The front plane of the model is shown in Fig. 1. A standard femur geometry was used to produce the finite element mesh of the cortical and cancellous bone. The "standardised femur" is the computer geometry model of a femoral bone analogue developed by the Laboratory for Biomaterials Technology of Istituti Ortopedici Rizzoli, Italy, within the frame of the Prometeo Project. The femoral analogue is produced by Pacific Research Labs (Vashon Island, Washington, USA). The previously meshed titanium alloy stem, the cement and the stem-cement and bone-cement interface were then inserted into the bone model. Femoral stem was positioned in the bone so that the head center of the prosthesis was located at the head center of the femur. The orientation of the implant in the bone was

dictated by the head center position and bone geometry. In order to account for the three-dimensional structural integrity of the bone, two side-plates were superimposed over the front plane. They were introduced in order to reproduce the integrity of the cortical bone and the cement, respectively. The non-uniform thickness pattern of the bone and cement was introduced in order to obtain the moment of inertia of the cortical bone and the stem in the finite element mesh equal to the real structure. The finite element analyses were performed making use of the finite element code ABAQUS (Hibbit, Karlsson and Sorensen, Inc., Pawtucket, RI). Only the stem-cement interfaces were activated during the analysis while the bone-cement interface was considered to be bonded throughout the finite element calculations. This study was in fact a preliminary step toward the evaluation of a realistic bone-cement interface model and no attempt was done in order to describe the interface behaviour in a finite element analysis of the implant system. The scope of the finite element analysis of the prosthesis implant was the evaluation of the stress distribution across the stem-cement and in particular, the bonded bone-cement interface. The study of the sensitivity of the load transfer mechanism to changes in stem geometry was out the scope of this paper. Moreover, because the usual stem materials (titanium or cobalt chromium) have an elastic modulus by two orders of magnitude larger than the adjacent cement and proximal cancellous bone, changes in stem material properties did not substantially change the load transfer mechanism between the stem and the cement. A sensitivity analysis was performed in this paper only with reference to the frictional coefficient of the stem-cement interface. The zero-thickness contact elements adopted in this study provide directly the normal and tangential stresses across both the stem-cement and bone-cement interfaces. The orientation of the hip-joint and greater trochanter force is indicated in Fig. 1.

A strenuous loading case, based on *in vivo* loading estimates for the stance phase of gait, was used as an estimate of loading in an active individual. The intensity of the prosthesis head loading P was 3200 N with an inclination on the vertical y axis equal to 12° (BERGMANN *et al.*, [1]). Muscle force Q was assumed acting on the greater trochanter with a total intensity of 2250 N and an inclination on the vertical y axis equal to 12° (BERGMANN *et al.*, [1]). The strenuous loading case was used since it represents a conservative design loading for younger, heavier and more active patients. The stem was titanium alloy with an elastic modulus of 110000 MPa. The elastic modulus of the PMMA was assumed to be equal to 2100 MPa, while the bone elements were isotropic with an elastic modulus equal to 18600 MPa for the cortical bone and 410 MPa for the trabecular bone. The Poisson ratio was equal to 0.25 for the materials. A total number of 1722 quadrilateral elements were used to generate the mesh reported in Fig. 1 while the total number of nodes were 1724. Moreover, 432 zero thickness contact elements were inserted to model the stem-cement and the bone-cement interface.

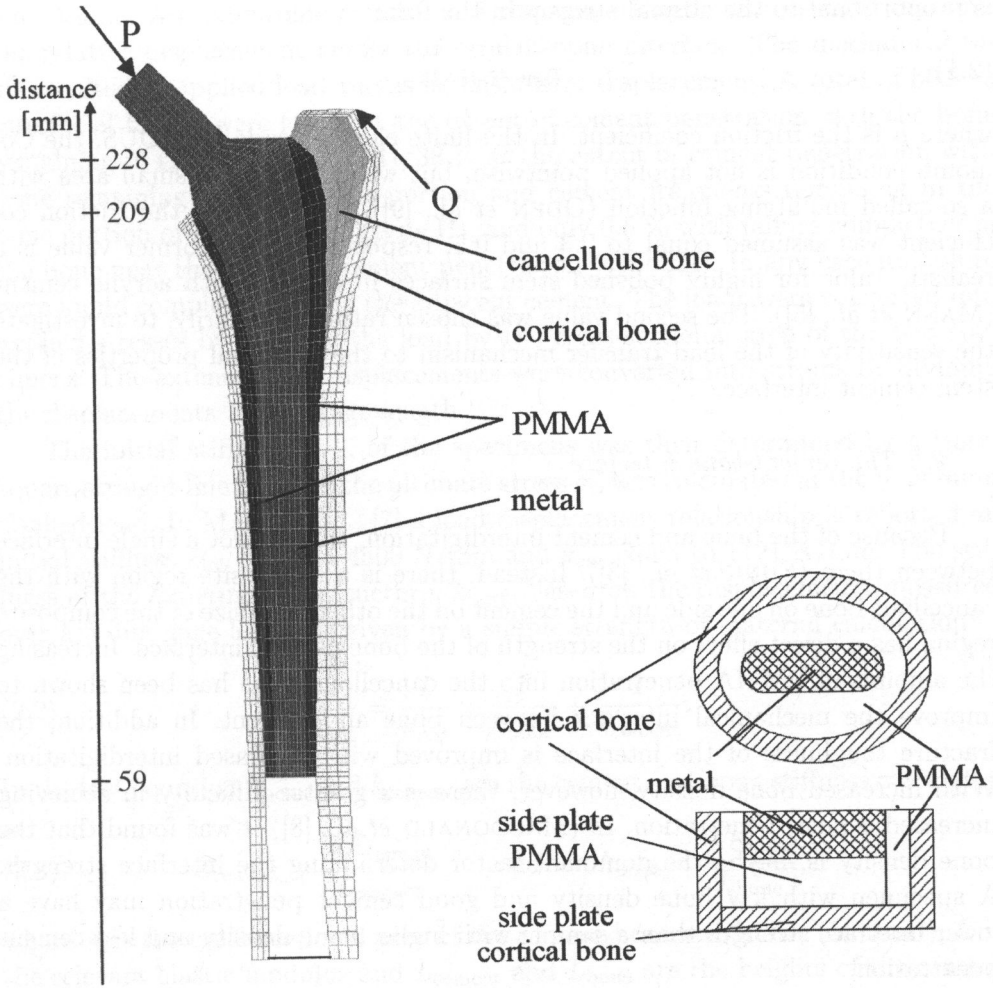

FIG. 1. Front plane of the finite element mesh. The elements of the front plane are of non-uniform thickness and were determined in such a way that the moment of inertia of the cortical bone, the stem and the PMMA in the finite element mesh were equal to the real structures. The cortical bone and the PMMA outside the front plane was modelled by a side plate.

2.1. The stem-cement interface

Zero thickness standard contact elements were used to model the stem-cement interface. When a Coulomb friction interface was adopted, the stiffness of the interface was very large in compression (bonded interface) and zero in tension (debonded interface). In shear, a Coulomb friction model was used. No relative motion occurs if the tangential stress τ is less than the critical stress τ_{crit} which

is proportional to the normal stress p in the form:

$$\tau_{\text{crit}} = \mu \cdot p, \tag{2.1}$$

where μ is the friction coefficient. In the finite element code ABAQUS, the Coulomb condition is not applied pointwise, but weighted over a small area with a so-called mollifying function (ODEN *et al.*, [9]). In this work the friction coefficient was assumed equal to 0.3 and 0.5, respectively. The former value is a realistic value for highly polished stem surfaces in contact with acrylic cement (MANN *et al.*, [5]). The second value was chosen rather arbitrarily, to investigate the sensitivity of the load transfer mechanism to the frictional properties of the stem-cement interface.

2.2 The cement-bone interface

Because of the bone and cement interdigitation, there is not a single interface between them (FUNK *et al.*, [3]). Instead, there is a composite region with the cancellous bone on one side and the cement on the other. The size of the composite region has a direct effect on the strength of the bone-cement interface. Increasing the amount of PMMA penetration into the cancellous bone has been shown to improve the mechanical interlock between bone and cement. In addition, the fracture toughness of the interface is improved with increased interdigitation. With increased bone density, however, there is a greater difficulty in achieving increased cement penetration. In (MACDONALD *et al.*, [8]) it was found that the bone density is maybe the dominant factor determining the interface strength. A specimen with low bone density and good cement penetration may have a lower interface strength than a sample with higher bone density and less cement penetration.

MANN *et al.*, [6] presented an experimental investigation to determine the general mechanical behaviour and in particular, the post-yield behaviour of the bone/cement interface under tensile loading. The cement-bone interface is capable of carrying substantial loading after the peak applied loading is reached due to the interdigitation between the cement and cancellous bone. Further, the post-yield softening behaviour under tensile loading has been shown to have an exponential type decay. Individual cement-bone test specimens were prepared for mechanical testing using a multistage approach including femur preparation, CT scanning, PMMA cementing and sectioning. A total of 71 cement-bone specimens (10-20 mm long, 10 mm wide and 5 mm deep) were included in the study. Different amounts of interdigitation were calculated from the CT scans (the mean value was equal to 1.54 mm and the standard deviation was equal to 0.89 mm). The specimens were tested at room temperature using a servo-hydraulic

load frame. An extensometer with a 5 mm gage length was used to measure the relative displacement across the cement-bone interface. The mechanical tests resulted in applied load versus extensometer displacement. A total of 56.5 % interfacial failure were found at the extent of cement penetration with the bone remaining in the cement (type I), 38 % at the extent of cement penetration with bone remaining in the cement portion and cement fragments remaining in the bone portion of the specimen (type II), and only 0.5 % with failure completely in the bone near the extent of cement penetration (type III). In any case no failure were found completely within the adjacent cement. The loads were converted into applied stresses by dividing the load by the cross-sectional area of the test specimens. The extensometer displacements were converted into strains by dividing the displacements by the gage length.

The initial stiffness, k_{int}, of the specimens was then determined by a least-square straight line fit while the ultimate stress σ_u was calculated at the maximum applied load. In MANN *et al.*, [7] a load-displacement relationship is reported an initial stiffness k_{int} equal to 4500 N/mm and k_{ext} equal to 1121 N/mm. The stiffness of the experimental structure, k_{kext}, based on the displacements measured over a 5 mm gage length is given by a simple strength of material calculation:

$$\frac{I}{k_{\text{ext}}} = \frac{I}{k_{\text{init}}} + \frac{I}{k_{\text{bone}}} + \frac{I}{k_{\text{cement}}}. \tag{2.2}$$

In the last equation k_{bone} and k_{cement} are the cement and bone stiffness calculated as

$$k_{\text{cement}} = \frac{AE_{\text{cement}}}{L_{\text{cement}}} \qquad \text{and} \qquad k_{\text{bone}} = \frac{AE_{\text{bone}}}{L_{\text{bone}}}, \tag{2.3}$$

where A is the cross-sectional area of the cement-bone specimens (50 mm^2), E is the relevant elastic modulus and L_{cement} and L_{bone} are the heights of the cement and bone segments within the 5 mm gage length, respectively. Both L_{cement} and L_{bone} were assumed equal to half the gage length (2.5 mm). Assuming an elastic modulus equal to 2100 MPa for the PMMA, k_{cement} will result equal to 42000 N/mm. From Eq. (2.2) the bone stiffness is then equal to 1547 N/mm which means an elastic modulus of the cancellous bone equal to 77 MPa (see Eq. (2.3)). From MANN *et al.* [6], the structural density of the cancellous bone close the interdigitation region showed a large dispersion and can be assumed to be equal to 500 mg/cm^3. Assuming then a bone density equal to 1500 mg/cm^3 (TURNER [11]), a reasonable value of the voids density is estimate equal to 30 %.

MANN *et al.* [6] recognised that the tensile failure of the interface occurs by failure of the trabeculae at the extent of cement penetration and that the strength is maximised by increasing the amount of trabecular bone in the cement. These findings suggest that the mechanism of trabecular bone failure is similar to the

interfacial failure. Then, a micro-mechanical model (COLOMBI *et al.* [2]) previously developed to study the tensile behaviour of bulk trabecular bone specimens, was used to reproduce the tensile test curve of the bone-cement interface. A finite element study was then performed making use of continuous damage mechanics concepts in order to address the softening behaviour of the bone-cement interface under tensile loading. A 2D finite element mesh of the trabecular microstructure was created according to COLOMBI *et al.* [2]. A grid of Voronoi polygons was defined as a function of some stochastic parameters, such as the number of polygons in the two directions x and y and the semi-length of the polygon edge. Subsequently, a shrinking of the microstructure was applied to reproduce the distribution and density of the pores within the matrix (30% in this particular case). The trabecular matrix was discretised making use of triangular 2D element and modelled as an isotropic material with symmetric behaviour in tension and compression. In this way, a 5×5 mm trabecular microstructure was obtained as indicated in Fig. 3a-c. The total number of nodes ranged from 759 to 773 while the total number of elements ranged from 1103 to 1270. Different amounts of interdigitation were then introduced as indicated in Fig. 3a-c by filling up the pores of the microstructure by PMMA and assuming a perfect bond between the PMMA and the bone.

A standard continuous damage model was used to model the softening behaviour of the bone under tensile loading. Since the experimental evidence shows that the mechanical failure of the interface is due to bone failure (MANN *et al.* [6], FUNK *et al.* [3]), in this work the cement elements were considered to be linear elastic throughout the analyses. In this preliminary step, an elastic-degrading model of the material stiffness has been assumed such that full unloading always leads to the origin (zero stresses and zero irreversible strains). This implies that no micro-crack closure-reopening effects are considered. Actually, for many materials and in particular for the bone, the reduction of stiffness was caused by the formation and propagation of micro-cracks. The stiffness degradation was defined directly in terms of degradation of the tangent stiffness tensor. In particular, a damage scalar model (SIMO *et al.* [10]) was used in which the non-linear behaviour of the material is determined by one damage variable d. The constitutive equation for the adopted damage model was isotropic because the stiffness degradation is described by a unique scalar factor d:

$$\boldsymbol{\sigma} = (1 - d)\mathbf{D}_0 : \boldsymbol{\varepsilon}, \tag{2.4}$$

where $\boldsymbol{\sigma}$ and $\boldsymbol{\varepsilon}$ are respectively the stress and strain tensor, d is the damage scalar variable, and $\mathbf{D}_0$ is the initial secant stiffness tensor. The damage threshold was defined by a loading condition:

$$F(\tau, d) = \tau - r, \tag{2.5}$$

where r is the current damage threshold and τ is an energy norm

$$\tau = \sqrt{\varepsilon : \mathbf{D}_0 : \varepsilon}. \tag{2.6}$$

The following damage evolution law was considered:

$$d(\tau) = 1 - \frac{\tau_0}{\tau} \exp\left[A\left(1 - \frac{\tau}{\tau_0}\right)\right], \tag{2.7}$$

where τ_0 and A are material parameters. With the above definition, the tangent operator takes the form (SIMO *et al.* [10]):

$$D_t = (1-d)\mathbf{D}_0 - \frac{\partial d}{\partial \tau} \frac{\sigma \otimes \sigma}{(1-d)^2 \tau}. \tag{2.8}$$

During the iterative procedure the energy norm is computed from the current total strain $\tau_{n+1}(\varepsilon_{n+1})$. Then if $\tau_{n+1} - r_n \leqslant 0$ (with $r_0 = \tau_0$) then $d_{n+1} = d_n$, otherwise $d_{n+1} = d(\tau_{n+1})$. The damage threshold is updated as $r_{n+1} = \max[r_n, \tau_{n+1}]$. The model depends on two material parameters τ_0 and A. The first one governs the onset of the damage phenomenon and is equal to:

$$\tau_0 = \frac{f_t}{\sqrt{E}}. \tag{2.9}$$

The parameter A is evaluated in order to impose that the same energy dissipation is always achieved independently of the mesh density and element size:

$$A = \left(\frac{G_f \cdot E}{l \cdot f_t^2} - \frac{1}{2}\right)^{-1}, \tag{2.10}$$

where E is the Young modulus, G_f is the fracture energy per unit area, f_t is the tensile strength and l is the finite element characteristic length. The condition $A \geqslant 0$ (the damage function must be monotonic and increasing) gives a limitation on the dimension of the finite element:

$$l \leqslant \frac{2 \cdot G_f \cdot E}{f_t^2}. \tag{2.11}$$

3. RESULTS

3.1. Stress distribution across the interfaces

The normal stress at the stem-cement and bone-cement interface is reported in Fig. 2a-d for the bonded and Coulomb friction interfaces.

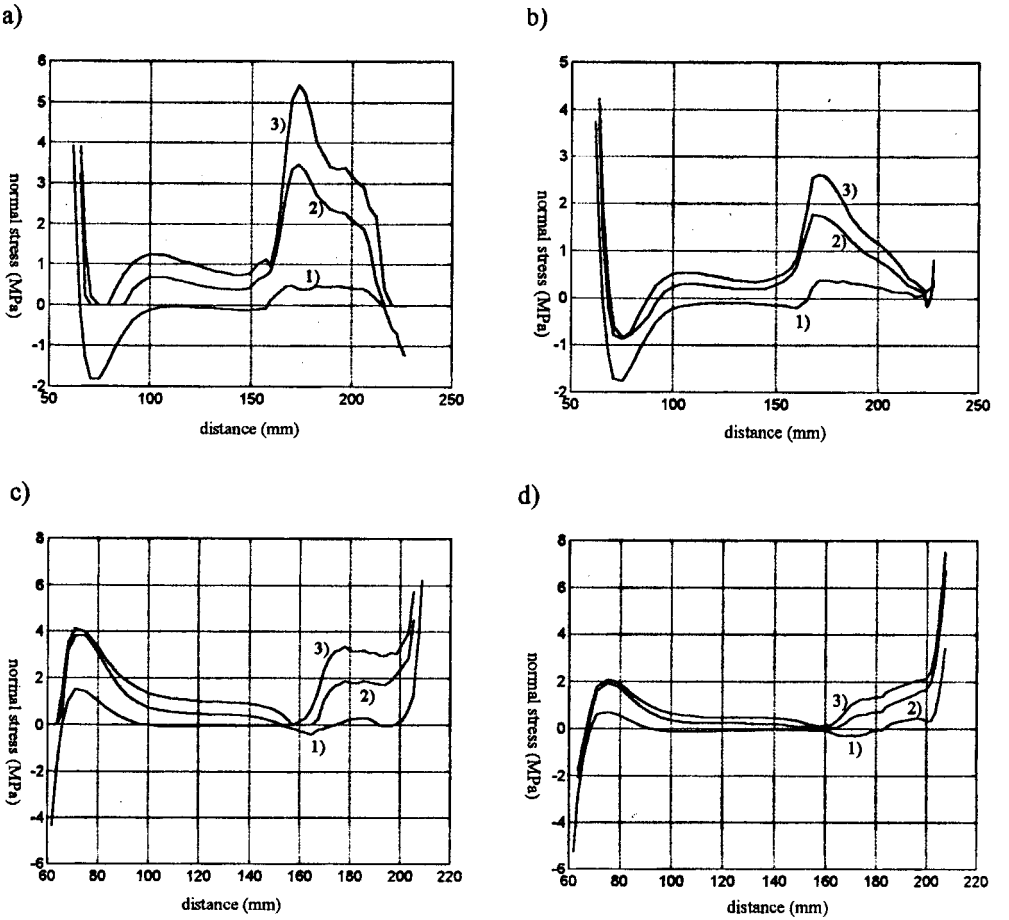

FIG. 2. Normal stress for different stem-cement interface condition (1) bonded interface, 2) $\mu = 0.5$ and 3) $\mu = 0.3$) at the: a) lateral side of the stem-cement interface; b) lateral side at the bone-cement interface; c) medial side of the stem-cement interface; d) medial side of the bone-cement interface.

At the lateral bonded stem-cement interface (see Fig. 2a), the distal stem worked as a beam on elastic foundation. In fact, due to the rotation of the stem, localised compressive stresses were present close to the tip, followed by a large tensile zone (the tensile peak stress was equal to 1.8 MPa). The normal stresses were equal to zero in the central stem since it had a straight shape and worked as a part of a composite beam (cortical bone + PMMA + stem) under axial load and bending moment (due to the orientation of the applied loads the shear load in this area was practically equal to zero). In the proximal stem, compressive normal stresses were present and finally, close to the collar region, tensile stresses were obtained (the tensile peak stress is equal to 1.2 MPa) again due to the rotation of

the stem. When a stem-cement frictional interface was adopted high compressive normal stresses were present in the proximal stem (see Fig. 2a) and then high circumferentially tensile stresses and radially directed cracks were expected in the cement mantle (JASTY *et al.* [4]). If a small stem-cement friction interface coefficient was adopted ($\mu = 0.3$), a significant increment of the peak compressive stress was recovered in the proximal stem.

A similar behaviour was present at the lateral bone-cement interface (see Fig. 2b). Again in the bonded stem-cement interface localised high compressive stresses were present close to the tip of the prosthesis followed by a large tensile zone (the tensile peak stress is equal to 1.8 MPa). In the central stem, the normal stresses were approximately equal to zero while in the proximal stem compressive stresses are present. In this case the muscles force applied to the trochanter prevents the formation of a tensile zone in the collar region. When friction was present between the stem and the bone, large compressive stresses were computed in the distal area but with a magnitude less then at the corresponding stem-cement interface (see Fig. 2a). Since the bone-cement interface was bonded in all cases, tensile stresses were present in the distal cement (the tensile peak stress was equal to 0.9 MPa). The value of this tensile peak stress was practically independent of the adopted stem-cement interface friction coefficient ($\mu = 0.3$ or $\mu = 0.5$).

At the medial bonded stem-cement interface (Fig. 2c), due to the rotation of the stem, a localised tensile zone (the tensile peak stress is equal to 4 MPa) was present at the tip of the prosthesis followed by a large compression zone. In the central stem, the stresses were equal to zero because the implant worked as a composite beam in the bonded case. In the collar region, the rotation of the stem produced localised compressive stresses. When a friction interfaces between the stem and the cement were assumed, high compressive stress were computed in the distal and in particular in the proximal stem. If small stem-cement friction interface coefficient is adopted ($\mu = 0.3$), a significant increment of the peak compressive stress is recovered in the proximal stem. Due to the high compressive normal stresses in the proximal and distal cement, high circumferential tension stresses and radially directed cracks are again expected in the cement mantle (JASTY *et al.* [4]).

A similar behaviour was present in the medial bone-cement interface (see Fig. 2d). In the bonded case, due to the rotation of the stem, localised high tensile stresses were present at the prosthesis tip (the tensile peak stress is equal to 5 MPa) followed by a large compressive zone. The normal stress in the central cement was again practically equal to zero while in the collar region, localised large compressive stresses were present. When friction was present at the stem-cement interface, a reduction of the tip peak tensile stresses to 2 MPa was observed.

This value was the highest tensile peak stress evaluated during this study at the bone-cement interface in a realistic situation of debonded stem-cement interface. Note that again the stress distribution in the distal cement was not influenced by the stem-cement friction coefficient.

3.2. Tensile behaviour of the bone-cement interface

Both the horizontal and vertical displacement were fixed on the bottom of the simulated bone-cement interface microstructure (see Fig. 3). Vertical displacements were then imposed on the top of the specimen and the relevant reactions were computed. Fig. 3a-c show the deformed microstructure of the bone-cement interface for different amount of interdigitation. The filled (black) bone element indicate the region with a damage greater than 0.9. Three amount of interdigitation were considered in this paper. In MANN *et al.* [6] the mean value of cement penetration was evaluated with a CT scan and was equal to 1.54 mm with a standard deviation of 0.89 mm. Since the total length of the simulated microstructure (see Fig. 3a-c) is 5 mm, the case reported in Fig. 3b was assumed to correspond to average interdigitation level.

With reference to this case, the parameters of the adopted damage model were calibrated as described in the previous section. In particular, in the previous section to match the initial stiffness of the experimental structure, the elastic bone Young modulus was computed equal to 77 MPa while the Young modulus of the PMMA was assumed to be equal to 2100 MPa (FUNK [3]). The Young modulus of the trabecular matrix was then roughly estimated by dividing the bone Young modulus by the voids density (30% for the microstructure reported in Fig. 3a-c). In this paper a slightly different value of 200 MPa was used in order to achieve a better fit of the experimental curve. In MANN *et al.* [7] it was reported a load-displacement relationship with a load peak equal to 70 N which correspond to a peak stress equal to 1.4 MPa (the area of the specimen was equal to 50 mm^2). This last value was used to produce a rough estimation of the tensile strength f_t of the bone matrix by simply dividing the peak stress by the voids density (30% for the microstructure reported in Fig. 3a-c). A slightly different value of 3.5 MPa was used in this paper to produce a better fit to the experimental data. From MANN *et al.* [2] the area under the load-displacement relationship (fracture energy) was estimated equal to 38 N·mm. A rough estimation of the fracture energy G_f per unit area is then computed by dividing this value by the area of the specimen. In this example, a slightly different value of G_f was assumed equal to 1 N/mm in order to produce a better agreement between the numerical results and the softening branch of the stress-strain relationship.

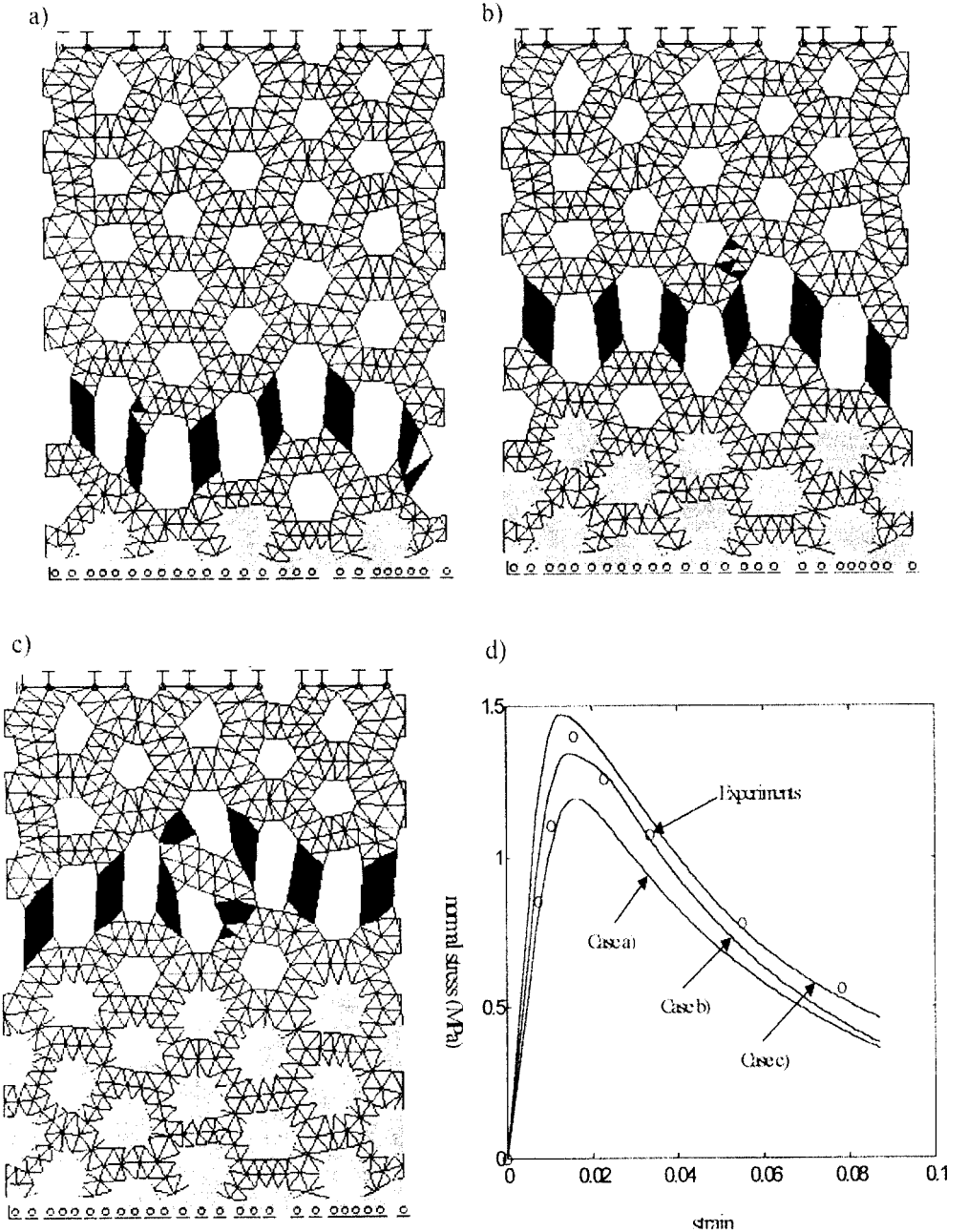

FIG. 3. a), b), c) deformed bone-cement interface microstructure for different amounts of interdigitation. The filled (black) bone elements indicate the region with a damage greater than 0.9. The interface failure was always at the extent of cement penetration with bone remaining in the cement half of the specimen (Type I interface failure); d) stress/strain relationship for the three different bone/cement interfaces under investigation (the experimental results from MANN *et al.* [6] are superimposed as circles).

The stress-strain relationships obtained with the estimated model parameter are reported in Fig. 3-d. The experimental results from MANN *et al.* [7] are superimposed as circles. As explained, the model parameter were estimated with reference to the interdigitation level of Fig. 3b. The relevant stress-strain curve is reported in Fig. 3-d as case b) and shows a good agreement with the experimental data from MANN *et al.* [7]. A reduction of the interdigitation level (see Fig. 3-a and case a) in Fig. 3-d) produced a reduction of 12% of the peak stress and a small amount of energy dissipation. On the other hand, an increment of the interdigitation level (see Fig. 3-c and case c) in Fig. 3-d) produced an increment of 10% of the peak stress and a greater amount of energy dissipation. In all these cases interfacial failure was found at the extent of cement penetration with bone remaining in the cement portion. The fracture zone is indicated in Fig. 3a-c as the filled (black) element and represent the most frequent, type I, interface failure as indicated in MANN *et al.* [6].

4. DISCUSSION

The goal of this study was to illustrate a preliminary step toward the investigation of the bone-cement interface condition in cemented total hip replacements in the early post-op period. In the literature, the bone-cement interface is usually assumed as bonded (MANN *et al.* [5]). In some cases a fibrous layer is assumed at the bone-cement interface (WEINANS *et al.* [12], JASTY *et al.* [4]) which produce a significant modification of the load transfer mechanism in the long-term implant. In this study no fibrous layer tissue was assumed in the analysis since clinical evidence shows that retrieved specimens at less than 5 years post-op have trabecular bone well interdigitated within the cement and no formation of fibrous tissue.

In the present study, a quasi-three-dimensional finite element analysis of the stem-cement and bone-cement interface condition of cemented femoral hip components was first performed. Both bonded and unbonded stem-cement interface condition was assumed in order to study the different load transfer mechanism. For the unbonded case, a Coulomb friction model was used and different values of the friction coefficient were assumed ($\mu = 0.3$ or $\mu = 0.5$) in order to investigate the sensitivity of the load transfer mechanism to the frictional properties of the stem-cement interface. The results in terms of normal stresses across the interfaces indicated a significant modification of the load transfer mechanism from the bonded to the unbonded case. The bone-cement interface was considered to be bonded trough the analyses and the effect of the frictional coefficient of the stem-cement interface was investigated. This study was in fact a preliminary step

toward the evaluation of a realistic bone-cement interface model and no attempts were done in order to describe the interface behaviour in a finite element analysis of the implant system.

On the bonded lateral side, a significant amount of tensile stresses were present in the distal stem-cement interface (see Fig. 2a) and a gap was then formed between the stem and the cement in the unbonded case. The corresponding stress redistribution at the interface gives a large amount of normal stresses in the proximal interface. A small friction coefficient ($\mu = 0.3$) produced a significant increment of the compressive peak stress in this area. Figure 2b indicates that tensile stresses were present in the distal bone-cement interface. The corresponding peak value was independent of the stem-cement interface condition. Again compressive peak stresses were present in the proximal interface with the peak stress strongly influenced by the stem-cement interface condition.

On the bonded medial side, a very high local tensile stresses were present close to the tip of the stem (see Fig. 2c). A local gap was then created between the stem and the cement in the unbonded interface. This produced a redistribution of the interface stresses with an increment of the compressive stresses in the distal and proximal interface. The peak stress in the distal interface was independent of the stem-cement frictional conditions while a reduction of the friction coefficient produce an increment of the peak stress in the distal interface. Figure 2d illustrates that local high tensile stresses was present at the tip of the stem in the bone-cement interface. The stress distribution was again independent of the stem-cement interface condition. Compressive stresses were present in the proximal cement with a strong dependence on the stem-cement interface conditions.

A finite element study was performed making use of continuos damage mechanics concepts in order to address the softening behaviour of the bone-cement interface under tensile loading. The parameters of the adopted damage model were calibrated by the experimental data of MANN *et al.* [6]. They found that under displacement-controlled tensile loading of the cement bone interface, there was no abrupt failure of cement-bone interface after the peak tensile stress is reached. Rather, a large amount of strain softening occurred at the cement-bone interface with a substantial energy absorption by the failing interface after the peak load was reached. The strain-softening behaviour of the bone-cement interface is similar in nature to the tensile behaviour found in the literature of bulk trabecular bone specimens (TURNER [11]). These findings suggest that the failure mechanism of trabecular bone is similar to the interface failure found in MANN *et al.* [6]. Therefore the continuum damage model used in COLOMBI *et al.* [2] to investigate the tensile behaviour of the trabecular bone was applied to study the bone-cement interface response. Different amount of bone-cement interdigitation

were considered in order to investigate the influence of this parameter on the tensile behaviour of the cement-bone interface. The results (see Fig. 3d) are in agreement with the experimental data and show a positive correlation between the tensile peak stress and the interdigitation level.

The highest tensile bone-cement interface peak stress obtained in the finite element analysis was equal to 2 MPa and was located at the tip of the stem on the medial side. This value was greater than the experimental tensile interface strength but was related to a narrow area close to the tip of the stem. A second large tensile stresses region was present on the lateral distal interface. The peak stress in this case was equal to 0.8 MPa and it was significantly lower than the tensile interface strength. These peak values was relative to an unbonded stem-cement interface since a firm and lasting bond between the stem and the cement mantle is difficult to realise clinically. A significant amount of tensile stresses were present only in a narrow region, and then it is difficult to understand the strong dependence of the structure stiffness from post-yield softening parameters postulated in MANN *et al.* [7]. Moreover, there was a substantial shear load transfer across the interface in the finite element model developed in this paper. Of interest was the observation in MANN *et al.* [6] that if aggressive endosteal bone reamers is used, a reduced amount of endosteal bone is available for cement-bone interdigitation. However, the actual behaviour of the bone-cement interface should include a shear or a combined normal and shear failure model (MANN *et al.* [7]). In this sense this paper is a preliminary step toward the study of a more realistic bone-cement interface model in the early post-op period.

ACKNOWLEDGEMENT

This research was supported by a grant from the Milan University of Technology. The authors would like to thank Prof. F. Bontempi of the University of Rome "La Sapienza" for his valuable help during the numerical computations.

REFERENCES

1. G. BERGMANN, F. GRAICHEN and A. ROHLMANN, *Hip joint loading during walking and running measured in two patients*, J. of Biomechanics, **26**, 969–990, 1993.

2. P. COLOMBI, R. CONTRO and M. PINI, *Modelling and analysis of the mechanical properties of trabecular bone*, ASME Winter Annual Meeting, BED, **36**, 131–132, 1997.

3. M.J. FUNK and A.S. LITSKY, *Effect of cement modulus on the shear properties of the bone-cement interface*, Biomaterials, **19**, 1561–1567, 1998.

4. M. JASTY, W.J. MALONEY, C.R. BRAGDON, T. HAIRE and W.H. HARRIS, *Histomorphological studies of the long-term skeletal responses to well fixed cemented femoral components*, J. of Bone Joint Surg., **72A**, 1220–1229, 1990.

5. K.A. MANN, D.L. BARTEL, T.M. WRIGHT and A.H. BURSTEIN, *Coulomb frictional interfaces in modelling cemented total hip replacement: a more realistic model*, J. of Biomechanics, **28**, 9, 1067–1078, 1995.

6. K.A. MANN, D.C. AYERS, F.W. WERNER, R.J. NICOLETTA and M.D. FORTINO, *Tensile strength of the cement-bone interface depends on the amount of bone interdigitated with the PMMA cement*, J. of Biomechanics, **30**, 4, 339–346, 1997a.

7. K.A. MANN, F.W. WERNER, D.C. AYERS, *Modelling the tensile behaviour of the cement-bone interface using nonlinear fracture mechanics*, J. of Biomechanical Eng., **119**, 175–178, 1997b.

8. W. MACDONALD, E. SWARTS and R. BEAVER, *Penetration and shear strength of cement-bone interface in vivo*, Clin. Orthop. Rel. Res., **286**, 283–288, 1993.

9. J.T. ODEN and E.B. PIRES, *Nonlocal and nonlinear friction laws and variational principles for contact problem in elasticity*, J. of Applied Mechanics, **50**, 67–76, 1983.

10. J.C. SIMO and J.W. JU, *Strain and stress-based continuum damage models* – I–II, Int. J. Solids and Structures, **23**(7), 821–869, 1987.

11. C.H. TURNER, *Yield behaviour of bovine cancellous bone*, J. of Biomechanical Engineering, **11**, 256–260, 1989.

12. H. WEINANS, R. HUISKES and H.J. GROOTENBORG, *Trends on mechanical consequences and modelling of a fibrous membrane around femoral hip prosthesis*, J. of Biomechanics, **23**, 10, 991–1000, 1990.

Received February 26, 1999.